JOURNAL OF VIROLOGY, July 1997, p. 5423–5431 Vol. 71, No. 7
0022-538X/97/$04.00+0

Comprehensive Quantification of Herpes Simplex Virus Latency at the Single-Cell Level

N. M. SAWTELL*

Division of Infectious Diseases, Children's Hospital Medical Center, Cincinnati, Ohio

Received 4 February 1997/Accepted 9 April 1997

To date, characterization of latently infected tissue with respect to the number of cells in the tissue harboring the viral genome and the number of viral genomes contained within individual latently infected cells has not been possible. This level of cellular quantification is a critical step in determining (i) viral or host cell factors which function in the establishment and maintenance of latency, (ii) the relationship between latency burden and reactivation, and (iii) the effectiveness of vaccines or antivirals in reducing or preventing the establishment of latent infections. Presented here is a novel approach for the quantitative analysis of nucleic acids within the individual cells comprising complex solid tissues. One unique feature is that the analysis reflects the nucleic acids within the individual cells as they were in the context of the intact tissue—hence the name CXA, for contextual analysis. Trigeminal ganglia latently infected with herpes simplex virus (HSV) were analyzed by CXA of viral DNA. Both the type and the number of cells harboring the viral genome as well as the number of viral genomes within the individual latently infected cells were determined. Here it is demonstrated that (i) the long-term repository of HSV-1 DNA in the ganglion is the neuron, (ii) the viral-genome copy number within individual latently infected neurons is variable, ranging over 3 orders of magnitude from <10 to >1,000, (iii) there is a direct correlation between increasing viral input titer and the number of neurons in which latency is established in the ganglion, (iv) increasing viral input titer results in more neurons with greater numbers of viral-genome copies, (v) treatment with acyclovir (ACV) during acute infection reduces the number of latently infected ganglionic neurons 20-fold, and (vi) ACV treatment results in uniformly low (<10)-copy-number latency. This report represents the first comprehensive quantification of HSV latency at the level of single cells. Beyond viral latency, CXA has the potential to advance many studies in which rare cellular events occur in the background of a complex solid tissue mass, including microbial pathogenesis, tumorigenesis, and analysis of gene transfer.

Unraveling the molecular interactions which underlie the establishment and maintenance of latent infections and periodic reactivation remains a major frontier in understanding and ultimately controlling herpes simplex virus (HSV). The ability to quantify viral burden at the level of single cells is essential for understanding many aspects of latency and reactivation. For example, the number of viral-genome copies within individual latently infected cells has been hypothesized to be central to the mechanism of reactivation by Roizman and Sears (29, 30) and Kosz-Vnenchak et al. (18). The inability to determine the number of latently infected neurons and the viral-genome copy number has made it impossible to discriminate between a role in establishment and a role in reactivation of genes which show a reduced reactivation phenotype (30).

Detection of the latency-associated transcript (LAT) RNA by in situ hybridization was the first approach used to mark latently infected neurons (6, 27, 28, 38–42). With respect to viral DNA, quantification of viral genomes in DNA harvested from latently infected ganglia was initially attempted by slot blot (21, 36). The application of PCR greatly increased the sensitivity of detecting the viral genome, and the quantitative assay developed by Katz et al. (16) represented a significant advance in the ability to measure the total amount of viral DNA in latently infected tissue. Modifications of this approach have been utilized by several investigators to quantify latency (8, 13, 26). Although it is a valuable measure, important information is lost in this analysis—namely, the number of cells which contain the viral genome and the number of viral-genome copies within individual latently infected cells. The increased sensitivity of in situ PCR has for the first time allowed detection of the latent viral genome in sectioned mouse ganglia (23, 25). Using this approach, Mehta et al. were able to demonstrate that more neurons contained the viral genome than contained detectable levels of LATs by in situ hybridization (25). Unfortunately, this critical advance does not include the means to quantify the number of viral genomes within individual latently infected cells.

Because of the potential importance of this parameter in the control of reactivation, we set out to develop an assay to quantify viral latency with respect to both the number of latently infected cells and the viral-genome copy number within individual latently infected cells. The approach was to transform the solid tissue into a single-cell suspension, to utilize a quantitative PCR assay to determine the number of latently infected cells within the dissociated tissue, and to quantify the number of viral genomes within the individual infected cells. The dissociation of living tissues is a well-established procedure (7, 48); however, the low recovery of adult neurons and the molecular changes triggered in cells during the dissociation made direct use of this approach undesirable. As detailed in this article, these problems were obviated by chemically stabilizing the tissue by fixation prior to dissociation. Presented here are data which demonstrate that this new method, called CXA (for contextual analysis), can be used to accurately and precisely quantify viral latency at the level of individual cells.

* Mailing address: Children's Hospital Medical Center, Division of Infectious Diseases, 3333 Burnet Ave., Cincinnati, OH 45229-3039. Phone: (513) 636-7880. Fax: (513) 636-7655. E-mail: Sawtn0@CHMCC ORG.

MATERIALS AND METHODS

Animals. Male Swiss Webster mice weighing 18 to 22 g (Harlan) housed in American Association for Laboratory Animal Care-approved facilities under National Institutes of Health guidelines were used for these studies.

Perfusion fixation and dissociation. Mice to be perfused were dosed intraperitoneally with 80 mg of sodium pentobarbital per kg of body weight and monitored for absence of pressure reflex. Deeply anesthetized mice were perfused by using a peristaltic pump, inserting the inflow needle into the left ventricle of the mouse, and clipping the right atrium or ventricle for outflow. Circulation of 20 ml of room temperature Streck's tissue fixative (STF) (Streck Laboratories, Inc.) was followed by 50 ml of fixative heated to 80°C. The tissues of interest were removed, finely minced, and placed in a solution of 0.25% collagenase (CLS I; Worthington) in Hanks balanced salt solution at 37°C. The tissue suspension was gently triturated, and the dissociation was monitored by microscopic examination of small aliquots. At completion, the dissociated tissue was gently pelleted, the collagenase was removed, and the pellet was resuspended in STF for a 15-min postfixation. Various lots of collagenase were screened for DNase and RNase activities and selected on the basis of the absence of nuclease activity.

Virus, inoculation, and replication kinetics. Stocks of HSV-1 strain 17syn+ (originally obtained from John Subak-Sharpe, Medical Research Council, Glasgow, Scotland) were generated and titered in rabbit skin cell (RSC) monolayers by routine procedures (44).

Anesthetized mice were inoculated by placing 10 μl of viral stock onto scarified corneas (34, 47). The acute phase of infection was monitored by determining the titers of virus in the eyes and the trigeminal ganglia (TG) in groups of three mice on the days indicated by a standard plaque titration assay on RSC monolayers.

Nucleic acid isolation. For DNA isolation, perfusion-fixed dissociated cells were pelleted and resuspended in a solution of 20 mM Tris and 20 mM EDTA, pH 7.4, containing 100 μg of proteinase K (Gibco BRL) per ml and 0.5% sodium dodecyl sulfate (SDS) and incubated at 55°C for 3 h (31). The samples were extracted with phenol-chloroform and precipitated with ethanol. For RNA, cell pellets were pulverized under liquid nitrogen and homogenized in Ultraspec RNA reagent (Biotecx) according to the manufacturer's specifications.

Immunohistochemistry. STF perfusion-fixed dissociated neurons harvested from TG were placed on glass slides (Superfrost Plus; Sigma) and air dried. Ganglia harvested from STF or 4% paraformaldehyde perfusion-fixed mice were dehydrated in graded ethanols and embedded in paraffin, and 8-μm-thick sections were picked up on glass slides. Slides were baked at 58°C overnight to facilitate adherence of tissue section to the slide. Paraffin was removed from sectioned ganglia in xylene and then washed in 100% ethanol. Slides containing sectioned ganglia and dissociated cells were rehydrated in phosphate-buffered saline (PBS), incubated in methanol containing 0.75% H_2O_2 for 15 min, rinsed in PBS, and subsequently incubated in PBS containing 5% nonfat dry milk and 0.2% Nonidet P-40 for 30 min. Rabbit anti-neurofilament 200 antibody (Sigma) was utilized in a standard three-step biotin-avidin-horseradish peroxidase assay as detailed previously (33).

Western blot analysis. Sample preparation, SDS-polyacrylamide gel electrophoresis, and Western blot analysis have been described in detail previously (20, 33, 46). In brief, equivalent volumes of fresh liver and perfusion-fixed dissociated liver cells were homogenized in Laemmli cocktail and boiled for 5 min. Lysates were loaded onto standard SDS–8% polyacrylamide gels, electrophoresed, and electrotransferred to nitrocellulose. Efficiency of transfer was monitored by visualizing transferred proteins with Ponceau S as described elsewhere (33). The nitrocellulose membrane was loaded into a Hoeffer blotting unit, and immunohistochemical detection of actin was carried out with monoclonal antibody C4 (kindly provided by J. L. Lessard), which recognizes cytoplasmic actin isoforms (22). Binding of C4 to the membrane was detected by incubating with biotinylated anti-mouse antibody diluted 1:500 (Vector Laboratories) followed by an avidin-alkaline phosphatase conjugate diluted 1:500 (Vector Laboratories). Visualization of complexes was carried out with the Vector Black substrate kit (Vector Laboratories) as directed by the manufacturer. A portion of the gel was stained with Coomassie blue to allow visualization of the full spectrum of proteins.

ACV treatment. Acyclovir (ACV) (Burroughs Wellcome) was administered intraperitoneally at a dose of 50 mg/kg three times/day for 6 days starting at the time of viral inoculation. Sterile saline was administered identically to control mice.

Gradient purification of dissociated TG. The Percoll (Pharmacia) gradient resulting in the cleanest separation of neurons from support cells was determined empirically. The pH of Percoll was adjusted to 6.0, and dissociated TG were layered onto 40/50/60 gradients and separated by centrifugation at 800 × *g* at 4°C for 10 min. The separation of TG neuronal populations was facilitated by heating the cell suspensions to 70°C for 15 min during the postfixation step, resulting in the separation of neurons at the 50/60 interface.

Neuronal cells were counted as follows. Aliquots were placed onto glass slides (Superfrost Plus; Sigma), air dried, and either counterstained with cresyl violet or assayed for neurofilament immunoreactivity as described above. The number of neurons in aliquots of the dissociated cell suspensions was determined by counting the number of cells morphologically consistent with being neurons which was confirmed on the basis of neurofilament immunoreactivity.

DNase treatment. Predictably, cell-free supernatants from dissociated latently infected ganglionic cells contained both HSV and mouse DNA detectable by PCR. DNase I added to purified cells resulted in loss of all amplifiable DNA in a time-dependent manner (see Fig. 3B), indicating that the free enzyme diffused into the fixed cells and destroyed the intracellular DNA. Selective elimination of extracellular DNA was accomplished by using DNase I covalently linked to beads (Mobitec). This immobilized DNase I contained no detectable free DNase I activity, as reported by the manufacturer and confirmed by spiking supernatants from the preparation with DNA. In contrast to treatment with DNase in solution, the immobilized DNase I-treated cell samples showed an initial reduction in levels of mouse DNA, which then remained stable even after an additional 24-h incubation with fresh enzyme (see Fig. 3B). When purified neurons harvested from uninfected TG were spiked with HSV DNA, treatment with immobilized DNase I resulted in the complete elimination of amplifiable HSV DNA (see Fig. 3B). Analysis of mouse DNA in these samples yielded the predicted signal intensity for the number of cells in the sample. These results demonstrate the ability to remove extracellular DNA (in this case, HSV DNA) while leaving the intracellular DNA (mouse genomic DNA) intact.

PCR analysis of DNA within perfusion-fixed dissociated cells. All reagents used were determined to be HSV and mouse DNA contamination free. Dissociated, gradient-purified neurons (or support cells) were rinsed in distilled H_2O, and aliquots were assessed microscopically for quantity and purity. Cells were counted as neurons on the basis of size and morphology (see Fig. 3A), which was confirmed in preliminary studies using immunohistochemical staining for neurofilament protein as a neuronal marker (see Fig. 1C). A portion of the cells was diluted so that the number to be analyzed was contained in a 1-μl volume. Ponceau S solution was added (1/200 volume) to the diluted cells. This dye, which stains the cells red, did not interfere with subsequent reactions and allowed visualization of the cells so that the precise number in each PCR tube could be determined microscopically prior to analysis. Immobilized DNase on polyvinyl beads (Mobitec) was resuspended in reaction buffer (20 mM Tris-HCl, 5 mM $MgCl_2$, 5 mM $CaCl_2$ [pH 7.5]) so that 5 μl contained 50 to 100 beads which were gently mixed into each 1-μl cells sample. The optimum number of DNase beads is determined for each batch of immobilized DNase by assaying for complete removal of amplifiable exogenous HSV DNA as described above. Samples were incubated at 37°C for several hours or overnight. (When cells were aliquoted at the single-cell level, many of the tubes contained no cells. Some of these tubes were employed as controls for the completeness of the DNase treatment.) Samples were placed in a PCR GeneAmp 2400 (Perkin-Elmer Cetus) and heated (94°C for 5 min) to inactivate the DNase. The temperature was reduced to 50°C, 34 μl of solution A (20 mM Tris-HCl [pH 8.4], 50 mM KCl, 4.5 mM $MgCl_2$, 50 μg of proteinase K per ml) was added to each sample, and the mixtures were incubated for 3 h. Standards were prepared and quantitated as described elsewhere (16, 35), and dilutions representing 10,000, 1,000, 100, 10, and 0 HSV genomes in 6 μl were treated identically to the way the cell samples were treated with the exception of the DNase treatment. Samples and standards were incubated at 94°C for 7 min to inactivate proteinase K and then at 63°C for the addition of 10 μl of solution B (20 mM Tris-HCl [pH 8.4], 50 mM KCl, 4.5 mM $MgCl_2$, 5% gelatin, 200 μM each deoxynucleoside triphosphate, 50 pmol of each primer [16]) and 1.25 U of *Taq* DNA polymerase (Gibco BRL) per reaction, for a total volume of 50 μl. Amplification parameters were 94°C for 30 s, 55°C for 30 s, and 72°C for 30 s for 40 cycles followed by a 7-min final extension at 72°C. Five microliters of each PCR product was electrophoresed through a 12% polyacrylamide gel, transferred to a nylon membrane (GeneScreen Plus), and probed with a ^{32}P-end-labeled oligonucleotide internal to the PCR primers as described elsewhere (16, 31, 35). The blots were exposed to a storage PhosphorImager cassette (Molecular Dynamics) and analyzed according to the manufacturer's protocol with ImageQuant software. Amplification of the viral genome with the ICP27 primers was performed as above with the exceptions that the $MgCl_2$ concentration was 2.5 mM and the annealing temperature was 60°C. The sequences of the ICP27 primers are as follows: forward, 5′ AAGATGTGCATCC ACCACAACC 3′; reverse, 5′ GCAATGTCCTTAATGTCCGCC 3′; internal, 5′ CCTTTCTCCAGTGCTACCTGAAGG 3′.

RESULTS

CXA: fixation/dissociation and the integrity of DNA, RNA, and protein in fixed cells after dissociation. The goal was to develop a method for the comprehensive quantitative analysis of latently infected tissue at the level of single cells. The approach was to transform the solid tissue into a single-cell suspension and utilize a quantitative PCR assay to determine the number of latently infected cells within the dissociated tissue as well as to quantify the number of viral genomes within the individual infected cells. In preliminary studies, well-established procedures for the dissociation of living tissue were utilized (7, 48); however, this approach proved to be inade-

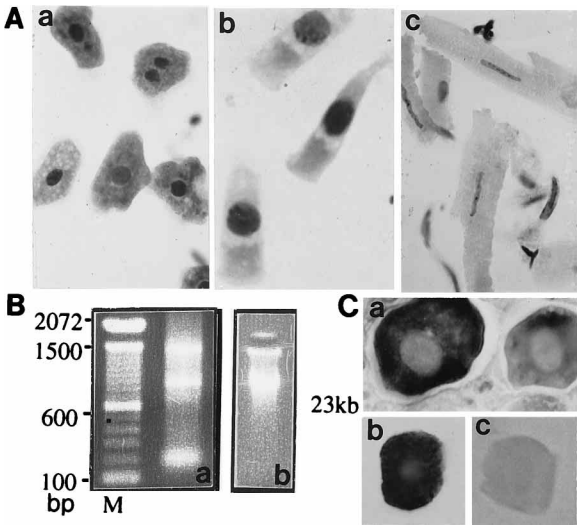

FIG. 1. (A) Photomicrograph of single-cell suspensions obtained from perfusion-fixed tissues. Mice were perfusion fixed with STF, and selected tissues were removed, minced, and dissociated in collagenase as detailed in Materials and Methods. Shown are perfusion-fixed liver (a), intestine (b), and heart (c) tissues after dissociation. The cell suspensions were dried onto glass slides, counterstained with cresyl violet, and mounted with Permount. (B) RNA and DNA isolated from perfusion-fixed dissociated cells. Routine isolation procedures were used to extract nucleic acids from perfusion-fixed tissue after dissociation (31). RNA (a) and DNA (b) samples were obtained from perfusion-fixed dissociated brain tissue and electrophoresed through standard ethidium-stained agarose gels. Lane M, size markers related to RNA. The DNA migrated above the 23-kb marker as indicated. (C) Immunohistochemical localization of neurofilament protein. Mice were perfusion fixed with STF, half of the ganglia were embedded in paraffin, and 8-μm-thick sections were cut on a rotary microtome. The remaining half was dissociated into a single-cell suspension, which was aliquoted and air dried onto glass slides as detailed in Materials and Methods. Both the paraffin-embedded fixed sectioned ganglia (a) and the dissociated perfusion-fixed ganglionic neurons (b) were examined for neurofilament protein by using a rabbit antibody specific for this protein. A standard three-step biotin-avidin-peroxidase immunohistochemical detection assay was utilized. (c) Rabbit serum control.

quate because of the low (10 to 20%) recovery of adult neurons and the molecular changes triggered in cells during the dissociation process. In an attempt to overcome these problems, the feasibility of dissociating tissues *after* chemical stabilization of fixation was tested.

Several common fixation formulations were tested in combination with alternative digestive enzymes. For the most part, the tissue either remained a solid mass or disintegrated into cellular debris. However, perfusion with STF followed by digestion with collagenase yielded single-cell suspensions from many solid-tissue types including peripheral and central nervous tissues, lung, liver, intestine, heart, pancreas, and reproductive tract. Microscopic examination of dissociated tissues showed that the vast majority of cells were morphologically intact (Fig. 1A). Analysis of DNA and RNA isolated from perfusion-fixed tissues after dissociation demonstrated that the nucleic acids within the cells were not significantly degraded during the process (Fig. 1B). By immunohistochemical staining, the distribution of cytoskeletal proteins including actin and neurofilament in dissociated cells was similar to that in sectioned tissue (Fig. 1C). There was no difference in the staining pattern in STF- or 4% paraformaldehyde-fixed sectioned material (not shown). Coomassie-stained SDS-polyacrylamide gels of lysates prepared from fresh liver and perfusion-fixed dissociated liver cells were also similar (Fig. 2). Western blot analysis for actin in lysates prepared from perfusion-fixed tissue after dissociation showed the predicted 43-kDa band with no apparent degradation (Fig. 2). These analyses demonstrated that perfusion-fixed tissues could be dissociated into morphologically intact single-cell suspensions and that the nucleic acids and proteins within the cells remained intact.

Using fixed dissociated cells to quantify HSV latency in TG. The mouse model of HSV corneal infection is a widely used animal model of HSV-1 infection (1, 4, 8, 18, 19, 23, 25, 29, 34, 35, 40, 41, 47) and was thus chosen for these studies. Inoculation at the corneal surface with HSV results in the establishment of latent infections in the TG (47). In preliminary experiments it was determined that perfusion-fixed TG could be dissociated into single-cell suspensions. The reproducibility of recovery of neurons from perfusion-fixed TG was determined by independently dissociating perfusion-fixed ganglia from each of five uninfected mice. Neurons were counted in aliquots of TG suspensions as detailed in Materials and Methods. The numbers of neurons recovered from the TG of different animals were found to be similar, ranging from 22,500 to 25,583 with an average of 24,117 ± 1,542 per ganglion or 48,234 ± 3,084 per ganglionic pair. This number is in the neighborhood of an estimate of 19,000 neurons/ganglion made from the analysis of sectioned mouse TG (5). However, another report of mouse TG estimated only 15,000/ganglion (10). The numbers given for rat TG are considerably higher, ranging from 25,000/ganglion (2) to 65,000/ganglion (3), and for cat the estimate is 11,000 to 18,000/ganglion (15). It is clear that there is considerable variation in the number of TG neurons estimated by different investigators examining the same species and an even greater variation among species. Although the absolute number of neurons in the mouse TG is not yet defined, these data demonstrate that similar numbers are recovered from different mice and that these numbers are not lower than estimates made from sectioned ganglia.

The dissociated TG suspensions contained single cells including neurons, satellite, and other support cells. Also present were tubular fragments (~200 μm) of myelin lined by very small cells which did not dissociate. Although the full spectrum of cell types capable of supporting HSV latent infections has not yet been determined, it is clear that the viral genome does reside within ganglionic neurons (6, 23, 25, 27, 28, 35, 38–42) and also reactivates in this cell type (24, 34). It was therefore desirable to obtain neurons separated from other cell types. As detailed in Materials and Methods, enriched populations of

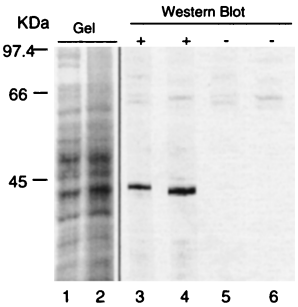

FIG. 2. Comparative analysis of proteins from homogenates of fresh tissue and perfusion-fixed dissociated tissue. Lanes 1 and 2, Coomassie-stained SDS–8% polyacrylamide gel of homogenates of fresh liver tissue and perfusion-fixed dissociated tissue, respectively; lanes 3 to 6, Western blot analysis of SDS–8% polyacrylamide gels of homogenates of fresh liver tissue (lanes 3 and 5) and perfusion-fixed dissociated tissue (lanes 4 and 6). Monoclonal antibody C4 which recognizes all actin isoforms (22) was used in lanes 3 and 4. Lanes 5 and 6, controls in which the primary antibody was omitted. There is strong immunoreactivity to a 43-kDa band in homogenates from both fresh liver tissue and perfusion-fixed dissociated liver cells.

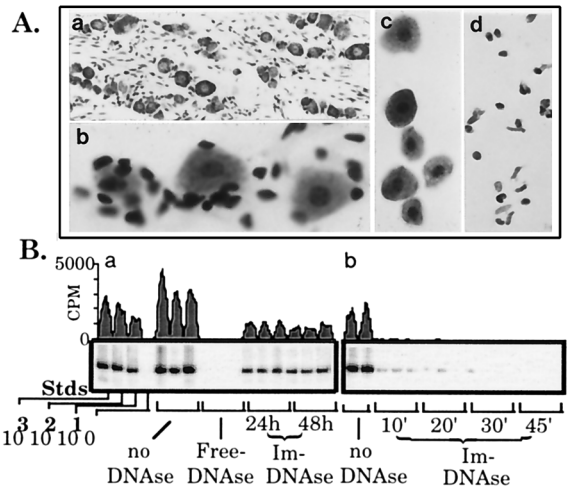

FIG. 3. (A) Photomicrographic series of the dissociation and gradient purification of perfusion-fixed TG. For comparative purposes, a section through a routinely processed paraffin-embedded TG counterstained with cresyl violet to emphasize the cellular components is shown (a). The ganglion is comprised of neurons (relatively large cells) and many small satellite/support cells. The architecture of the ganglia and the relationship between neurons and satellite cells becomes apparent during the dissociation of perfusion-fixed minced ganglia. Sampling during the dissociation process and examination of whole cells following cresyl violet staining reveals satellite cells peeling away from ganglionic neurons (b). After dissociation, cell populations were separated on Percoll gradients as detailed in Materials and Methods. Aliquots of perfusion-fixed dissociated and gradient-purified neurons (c) and satellite/support cells (d) are shown at the same magnification and are representative of samples analyzed by PCR. (B) Selective removal of extracellular DNA. (a) Triplicate samples each containing 10 purified neurons (see panel c above) (harvested from the TG of perfusion-fixed uninfected mice) were treated with no DNase, free DNase, or DNase immobilized on beads (Im) as indicated. Following treatment, PCR amplification of the single-copy mouse adipsin gene was carried out on these samples and standards (Stds) representing 1,000, 100, 10, and 0 diploid mouse genomes (16, 35). Note that fresh Im DNase was added at 24 h to samples incubating for 48 h. (b) HSV DNA representing 500 viral-genome copies was added to samples each containing 10 purified neurons (harvested from uninfected mice). Spiked samples were left untreated (first two lanes) or were treated with Im DNase, and the samples were incubated at 37°C for the times indicated (in minutes). Following treatment, PCR amplification of the HSV TK gene was carried out as described elsewhere (16, 35). ImageQuant software was used to generate the tracings of the blots shown.

neurons or satellite/support cells were obtained by separating the perfusion-fixed dissociated cells on Percoll gradients (Fig. 3A). Cells such as those shown in Fig. 3A could now be obtained from latently infected tissue and analyzed by quantitative PCR for the viral genome to determine both the number of latently infected cells and the viral-genome copy numbers within individual latently infected cells.

Before the analysis of latently infected ganglia, the issue of extracellular DNA contamination needed to be addressed. The principal goal was to develop a system which yielded information on the DNA contents of selected groups or individual cells dissociated and purified from a heterogeneous population. Therefore, DNA released from cells during the dissociation process or introduced from exogenous sources needed to be eliminated prior to analysis. This was accomplished by using DNase I covalently linked to beads as detailed in Materials and Methods. As shown in Fig. 3B, this treatment resulted in the removal of amplifiable extracellular DNA while leaving intracellular DNA intact.

Localization of viral genomes. On the basis of in situ hybridization for LAT RNAs, it has been concluded that the neuron is the site of HSV-1 latency (6, 27, 28, 38–42). More recently *in situ* PCR for HSV DNA, an assay shown to mark more latently infected neurons than those containing detectable LATs, has upheld this conclusion (25). However, the intimate physical association between neurons and satellite cells and the disparate sizes between the two cell types could easily result in failure to recognize a positive signal from satellite cells in sectioned ganglia. Utilization of dissociated TG cell populations provided the opportunity to screen large numbers of cells by PCR for the viral genome. Because positive signals would be detected by probing the PCR products, the potential difficulties in interpreting signals on sectioned material would be circumvented. Therefore, we used CXA to examine which ganglionic cell types harbored latent viral DNA (CXA-D).

Mice which had been inoculated via corneal scarification with 2×10^3 PFU of 17syn+ at least 30 days before were perfusion fixed, and the TG were dissociated as described above. Dissociated TG cell suspensions from groups of six latently infected ganglia were separated into neuron and satellite/support cell populations on Percoll gradients. Samples containing 20 neurons or >100 support cells were analyzed for HSV DNA as detailed in Materials and Methods. Ninety percent (9 of 10) of the neuron samples but none of the support cell samples (0 of 10) were positive for the viral genome (Fig. 4A). These findings indicated that the latent viral genome was predominantly within neurons. In order to more completely assess the distribution of viral genomes in latently infected ganglia, the remaining fractions from the Percoll gradients as well as unfractionated TG cell suspensions were analyzed. Samples were characterized with respect to the number of cells

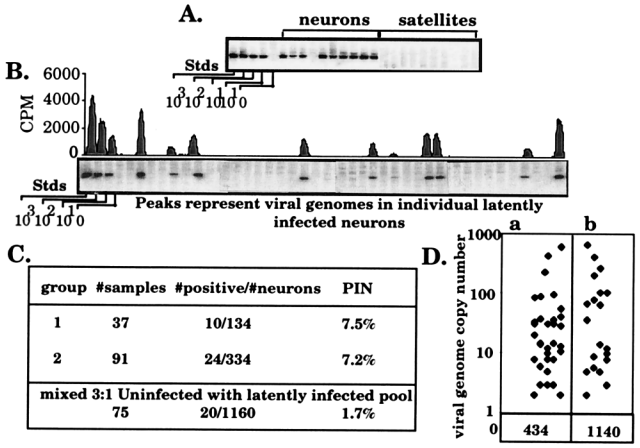

FIG. 4. (A) Cellular distribution of viral genomes in latently infected ganglia. Neuron and satellite cell populations were harvested from a sample of six latently infected perfusion-fixed ganglia as described in Materials and Methods and analyzed for the HSV genome by PCR using the viral TK primers (16, 35). Shown are the HSV TK PCR products amplified from samples containing 20 neurons each (see panel c in Fig. 3A) or >100 support cells each (see panel d in Fig. 3A). Also shown are the standards (Stds) representing 1,000, 100, 10 (duplicate samples of this standard were amplified), and 0 HSV genomes amplified along with the samples. (B) PIN. Additional neurons from the group in panel A were aliquoted (three or four per sample) and analyzed for HSV DNA as described in Materials and Methods. Shown are the HSV TK PCR products amplified from 40 samples of three or four neurons each and HSV standards. The densitometric tracing emphasizes the variability in the number of genome copies within individual latently infected neurons. (C) Summary of CXA-D analysis of latently infected neurons. The total numbers of samples, the total numbers of neurons contained within these samples, the numbers of positives, and the PINs are listed. The results of adding uninfected neurons to this pool of latently infected neurons are also summarized. (D) Viral-genome copy numbers in individual latently infected neurons before (a) and after (b) mixing with uninfected neurons. The viral-genome copy number in each positive neuron was calculated by comparing the counts per minute in the sample to the standard curve. Each symbol represents a single positive neuron. The numbers of negative neurons appear at the bottom.

and presence of neurons as described in Materials and Methods. Detection of viral DNA correlated with the presence of neurons. Cell samples devoid of neurons were negative despite the presence of large numbers of other cell types (0 of 13 samples with >500 cells each). Very rarely a sample of a large number of satellite/support cells was HSV positive (data not shown). There are three possible explanations for this observation: (i) a very rare HSV DNA-containing satellite cell (<1 in 10,000), (ii) incomplete removal of contaminating extracellular DNA, or (iii) an undetected contaminating neuron. We cannot rule out any of these possibilities. However, the otherwise strict segregation of viral genomes to neurons would suggest that an undetected contaminating neuron is the most likely explanation. The fact that under certain inoculation conditions one in three neurons was found to contain the viral genome whereas the number of viral genomes detected in cell samples devoid of neurons remained very low (<0.1% of cells) indicates that the vast majority of latent HSV-1 resides within neurons. It should be noted that the restriction of viral genomes to the neuronal population is not due to an inability to detect the DNA in nonneuronal cells, since prior to day 10 postinfection (p.i.), HSV DNA was detected in the satellite/support cell population (data not shown).

Frequency of HSV DNA-containing neurons. The use of CXA-D to determine the percentage of infected neurons in the ganglia was next tested. Since all but 1 of the 20 neuron samples were positive, the number of neurons per tube was reduced to three or four. Subsequent analysis demonstrated that if a sample was positive, there was a 90% chance that there was only one positive neuron in the sample. Two groups were analyzed independently. The first group included 37 samples (13 with three neurons and 24 with four neurons). Ten of the 37 samples (134 neurons) were HSV DNA positive, indicating that the percentage of infected neurons (PIN) in these ganglia was 7.5% (Fig. 4B and C).

The second group included 81 samples (36 with three neurons and 45 with four neurons). Twenty-one of the 81 samples (288 neurons) or 7.3% of the neurons were positive, in close agreement with the PIN of 7.5 obtained for the first group (Fig. 4C). This number is significantly higher than the estimates of 1% obtained by the most commonly used measure, in situ detection of the abundant LAT RNA (1, 29, 38). However, it is closer to the estimate of 4.8% generated by in situ PCR analysis of viral DNA (25). As is demonstrated in this report, depending on the virus, the input titer, and the extent of viral replication, the number of neurons in which latency is established can span a wide range, from <1 to 30%. Thus, a direct comparison of CXA-D and in situ PCR analyses would be required to determine the relative sensitivities of these two methods for determining the number of latently infected neurons.

Viral-genome copy number within individual neurons. By comparison to viral-genome standards, it was evident that the number of viral genomes contained within individual latently infected neurons ranged over 3 orders of magnitude, from <10 to 1,000 (Fig. 4B and D). In order to determine whether this reflected a real difference in the number of viral-genome copies within individual latently infected neurons or merely the level of variability inherent in the assay, CXA-D for the single-copy mouse adipsin gene was performed on 11 samples containing 10 perfusion-fixed dissociated mouse cells each to determine reproducibility. Comparison to mouse genomic DNA standards revealed a mean diploid copy number of 9 per sample with a range of 5.2 to 10.3. Thus, the fact that the number of viral genomes in individual latently infected cells ranged over 3 orders of magnitude could not be attributed to variability in the assay.

It was important at this point to establish (i) that what was being measured was viral DNA *within* cells, (ii) that the assay was reproducible, and (iii) that the results obtained accurately quantified ganglionic latency. In order to address the first issue, a mixing experiment was performed. The prediction was that if the viral DNA being measured was actually within cells, then mixing neurons from latently infected ganglia with neurons from uninfected ganglia should result in a reduction in the number of latently infected neurons in the population. The number of viral genome copies within those neurons which were latently infected, however, should remain the same. Neurons purified from perfusion-fixed uninfected ganglia were mixed with the latently infected pool of neurons in a ratio of 3:1 with the expectation of reducing the number of HSV-containing neurons in the population fourfold. The PIN of the mixed population was reduced by a factor of 4.25, from 7.4 to 1.7% (20 of 1,160 neurons, analyzed in 75 samples [40 samples with 15 neurons each and 35 with 16 neurons each) (Fig. 4C). The range of viral-genome copies within the individual infected neurons, however, did not change (Fig. 4D), indicating that the quantal distribution of viral DNA being measured within the cell population was stable. An additional mixing experiment was performed in which perfusion-fixed uninfected and latently infected ganglia were minced, dissociated, and purified together. Again, the PIN in the mixed group was reduced from that of the latently infected ganglia harvested from the same group of mice as predicted. The range of viral-genome copy number within individual latently infected neurons was similar (data not shown).

Reproducibility of the assay. In order to test the reproducibility of the assay, at >30 days p.i., mice inoculated via corneal scarification with 10^6 PFU of TB, a 17 syn+ based thymidine kinase-negative (TK^-) mutant, were perfusion fixed, and the TG were dissociated. TB was utilized because preliminary experiments demonstrated that when inoculated on the cornea, this TK^- mutant established fewer latent infections, making it possible to analyze neurons in groups of 10 rather than individually. In this experiment, three groups of three mice each were analyzed independently. In addition, the number of latently infected neurons in one group of mice was determined in three independent analyses. The three groups of mice had similar numbers of latently infected neurons: 3.7, 3.1, and 3.7% (6 of 180, 5 of 160, and 7 of 190, respectively). Independent analyses of a single group were also similar: 3.3, 4.0, and 3.9% (6 of 180, 8 of 200, and 7 of 180, respectively). The variation within and among groups was not significant ($P = 0.998$).

Accuracy of the assay. The accuracy of the assay in quantifying ganglionic latent infections was addressed through the following questions. (i) Was the frequency of latently infected neurons in the entire ganglionic neuronal population similar to that in enriched neuronal population? (ii) Did the region of the viral genome chosen for amplification bias the results? (iii) Was the total number of viral DNA molecules determined from the frequency and genome copy number profile obtained through CXA-D similar to the number determined by the whole-ganglion PCR assay developed by Katz et al. (16)? Finally (iv), Did the assay reflect predicted changes in the establishment of latent infections resulting from manipulations of input titer or viral replication?

In order to determine whether the number of latently infected neurons in the Percoll gradient-enriched neuronal population represented that for the entire ganglionic neuronal population, neurons from all parts of the gradient were analyzed for viral DNA. At 30 days p.i., mice which had been

TABLE 1. Effect of input titer on PIN

Input PFU[a]	PFU/TG pair[b]	No. of infected neurons (PIN)
4×10^3	1.6×10^4	8/75 (10.6)
4×10^4	1.4×10^4	21/88 (23.9)
4×10^5	1.6×10^4	25/82 (30.5)
4×10^6	6.0×10^4	18/63 (28.6)

[a] Total number of PFU placed on scarified corneas.
[b] Peak titers in all groups were reached on day 4 p.i. and are reported as the average PFU per TG pair.

inoculated via corneal scarification with 4×10^4 PFU of strain 17syn+ were perfusion fixed, and the TG were dissociated. In aliquoting samples, only the number of neurons per tube was taken into consideration. Single-*neuron* samples were analyzed. However, from most portions of the gradient, the samples contained many other cells in addition to the single neuron. The results demonstrated that utilizing the enriched neuron population did not bias the results. Twenty percent (32 of 160) of the neurons analyzed from the enriched neuronal population, compared to 18% (46 of 256) of neurons from other regions of the gradient, contained the viral genome. There is no statistically significant difference between these numbers.

In order to test the possibility that the region of the viral genome being amplified resulted in an over- or underrepresentation of the number of latently infected neurons, primers corresponding to a portion of the ICP27 coding region were selected. The percentage of latently infected neurons determined with the ICP27 primers, 18% (18 of 98), was not different from those obtained in analysis with the TK primers, 20 and 18%. These findings demonstrated that amplification of two distinct regions of the viral genome resulted in the same percentage of latently infected neurons. Thus, the PIN obtained was independent of the region of the genome being amplified.

The amplification of the viral genome from DNA isolated from whole ganglia is frequently used to quantify the number of viral DNA molecules in the ganglia (8, 13, 16, 19, 35). A direct comparison of the value obtained from this method with that obtained by CXA-D is not possible. However, a group of latently infected mice was analyzed, using both methods. Mice were inoculated with 10^6 PFU of the TK^- mutant, and at 30 days p.i., ganglionic pairs harvested from three mice were individually processed for whole-ganglion PCR as described elsewhere (35). Perfusion-fixed ganglia from additional mice were analyzed by CXA-D. The PIN was determined to be 3.7% (54 of 1,470) (see "Reproducibility of the assay" above) with an average of 25 copies/positive neuron. With 20,000 as the number of neurons per ganglion (5), the total number of viral DNA molecules per ganglionic pair would be 3.7×10^4, comparing well with the average value obtained by using whole-ganglion PCR, $3 \times 10^4 \pm 2 \times 10^4$. This value also compares well with the value reported by Katz et al. (16) for two other TK^- mutants.

Input titer and the establishment of latency. A simple and testable hypothesis is that increased viral input titer would result in an increased number of latently infected neurons. In order to test this, mice (20 per group) were inoculated with a total of 4×10^3, 4×10^4, 4×10^5, or 4×10^6 PFU of 17syn+ on scarified corneal surfaces. Eyes and TG were harvested from three mice per group on days 2, 4, and 6 p.i., and the levels of infectious virus were determined. As measured by a standard plaque titration assay, the acute replication kinetics for the four input titers were similar. TG titers were greatest on day 4 in all groups, with a maximum difference between titers of about fourfold (Table 1). At day 30 p.i., three mice from each group were perfusion fixed, the TG were harvested, and the numbers of neurons containing viral DNA and the viral-genome copy numbers in individual latently infected neurons were determined by CXA-D. As summarized in Table 1, the number of latently infected neurons ranged from 10.6% for the lowest input titer to 30.5% for the group receiving 2 orders of magnitude more virus. The differences between the numbers of latently infected neurons in the lowest- and two highest-input-titer groups achieved statistical significance ($P = 0.0195$ and $P = 0.033$, respectively; Fisher's exact test). The number of genome copies in the latently infected pool of neurons resulting from each input titer is shown in Fig. 5. If latently infected neurons are grouped on the basis of viral-genome copy number into low (<10)-, medium (10 to 100)-, and high (100 to 1,000)-copy-number neurons, the percentage of neurons residing within the medium- and high-copy-number groups increases with increasing input titer.

DNA replication and the establishment of latency. ACV class drugs have been shown to reduce viral replication at the surface and in the ganglia when administered to mice during acute infection (11, 12, 17, 43). This treatment has also been shown to affect the number of ganglia which reactivate by explant cocultivation (11, 12, 17, 43). However, the effect on the establishment of latency has not been directly quantified. ACV was administered to mice during the acute infection in order to determine the impact of reduced viral replication on the number of latently infected neurons in the TG and their viral-genome copy number. Two groups of 20 mice each were inoculated with 4×10^4 PFU of 17syn+. Starting at the time of inoculation, one group of mice was treated with 50 mg of ACV per kg administered three times a day intraperitoneally for 7 days, and the second group received sterile saline administered identically. Tissues (TG and eyes) were harvested from three mice per group for replication kinetics on days 2, 4, and 6 p.i., and levels of infectious virus were determined. As predicted and as shown in Fig. 6, ACV treatment significantly reduced the titers of infectious virus recovered from both the eyes and TG. At 30 days p.i., three mice from each group were perfusion fixed, the TG were dissociated, and the number of latently

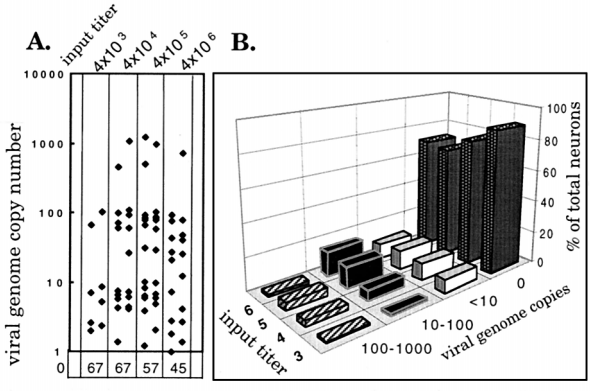

FIG. 5. Viral-genome copy numbers in individual latently infected neurons. (A) Scattergram of the viral-genome copy number in individual latently infected neurons from groups of mice inoculated with the input titers indicated. The copy number was calculated from counts per minute of the individual sample and a standard curve generated from samples containing known quantities of HSV DNA amplified with each group of single-neuron samples. (B) Relationship between the input titer (3, 4×10^3; 4, 4×10^4; 5, 4×10^5; 6, 4×10^6) and the percentage of the total number of neurons in the latently infected ganglia containing 0, <10, 10 to 100 or 100 to 1,000 viral-genome copies.

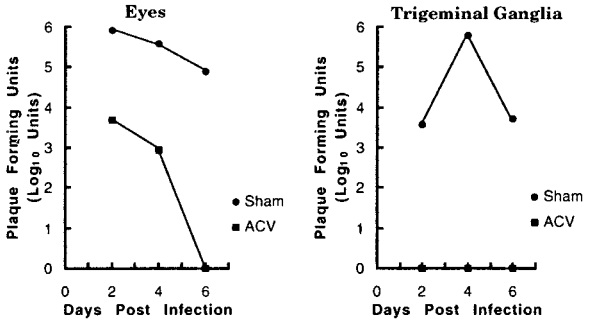

FIG. 6. Viral replication in eyes and TG in sham- and ACV-treated mice. Titers were determined in homogenates of tissues harvested from three mice from each group. Tissues were homogenized in 1 ml of medium. The data are PFU per milliliter of tissue homogenate.

infected neurons was determined for each group of six ganglia as described above. The number of latently infected neurons was dramatically reduced in the ACV-treated group compared to the saline-treated controls. While 20% (32 of 160) of the neurons in the sham-treated mice contained the viral genome, only 1.1% (16 of 1,411) of neurons in ACV-treated mice were positive ($P < 0.00001$). The number of viral genomes within the pool of latently infected neurons was also dramatically altered, with all of the positive neurons in the ACV-treated mice containing <10 viral-genome copies compared to the 3-log range in viral-genome copies in neurons harvested from the saline-treated controls (Fig. 7).

DISCUSSION

In this article it has been demonstrated that CXA-D can be utilized to reproducibly quantify the number of latently infected neurons within the ganglia as well as the viral-genome copy number within individual latently infected neurons. This is the first analysis which quantifies both of these aspects of HSV latency. In order to validate the assay as a precise and accurate measure of HSV latency at the single-cell level, the following facts were established. (i) The dissociation of fixed tissues yielded single cells with intact DNA, RNA, and protein. (ii) The yields of neurons from fixed dissociated TG were consistent from mouse to mouse. The fact that our yields were 10% greater than the highest estimates from sectioned mouse ganglia (5, 10) demonstrated that significant numbers of neurons were not being lost during the dissociation process. (iii) The recovery of neurons in the enriched fraction of the Percoll gradient was 30 to 40% of the input neurons. The analysis of neurons in other portions of the gradient demonstrated that this was a representative population with respect to latent viral genomes. (iv) With immobilized DNase I, amplifiable extracellular DNA was eliminated but the intracellular DNA was left intact. (v) Mixing uninfected and latently infected ganglia or purified neurons in given ratios reduced the PIN as predicted. (vi) Analysis of a given pool of latently infected neurons using two different primer sets from physically distant regions of the viral genome gave the same percentage of infected neurons. (vii) There was no statistically significant difference in the PINs obtained from multiple analyses of the same pool of neurons or the analyses of pools of neurons harvested from different mice of the same inoculation group. (viii) In a comparison using a TK^- mutant, the viral-genome copy number determined by whole ganglion PCR and that estimated from the PIN and average viral-genome copy number were similar. With the wild-type strain, calculations of the total viral-genome burden using the PIN, the average number of viral genome copies per neuron, and the estimated 20,000-neurons/ganglion yield values of 10^5 to 10^6 viral genomes, comparing well with the range reported by other investigators using whole-ganglion quantitative PCR (8, 16, 19, 35). In addition, several experimental conditions were devised in which a logical predicted outcome could be tested. As discussed below, the results of these experiments further supported the conclusion that CXA-D was accurately measuring ganglionic latency.

Our findings support and extend previous findings which have indicated that neurons are the repository of latent HSV-1 genomes (6, 23, 25, 27, 28, 35, 38–42). CXA-D allowed a more exhaustive analysis of nonneuronal cell types in the ganglia and eliminated the difficulties in interpreting the origin of signals on sectioned material. If support cells contain viral genomes, it is an extremely rare event. Alternative interpretations of the rare-positive support cell samples have been discussed. One additional possibility is that these represent not latent viral DNA but the very restricted spread of virus produced during a spontaneous reactivation. Analysis of the number of positive support cells before and after induced reactivation may shed some light on this matter.

The standard inoculation route (corneal scarification), strain (17syn+), and input titer (5×10^4 PFU) resulted in the establishment of latent infections in ~20% of the neurons in the ganglia. This is fourfold higher than the 4.8% estimated by in situ PCR. This could reflect differences in the sensitivities of the two methods. Since only 48% of the cells known to contain a diploid mouse gene were positive by in situ PCR, low viral-genome copy number latency could go undetected (25). However, variation in the strain of mouse and the input titer may also account for the difference observed. It is clear that a direct comparison of in situ PCR and CXA-D is required to determine the relative sensitivities of the two procedures (32a).

Although it has been demonstrated that viral replication is not essential for the establishment of latency (9, 37), there is significant evidence that the amount of virus, either as input PFU or as a result of surface replication, is involved in determining the total latent ganglionic viral-genome burden (discussed in reference 14). By experimentally manipulating viral replication, input titer, and viral strain or specific mutant (44), the number of latently infected neurons was found to range from 1 to 30% or from 200 to 6,000 neurons/ganglion. It was

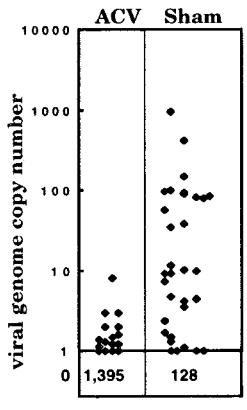

FIG. 7. Scattergram of the viral-genome copy numbers in individual latently infected neurons harvested from groups of mice treated during acute infection with ACV or saline. The copy number was calculated from the counts per minute of the individual sample and a standard curve generated from samples containing known quantities of HSV DNA amplified with each group of single-neuron samples.

predicted that the outcome of varying input titer or reducing viral replication would be reflected in a change in the number of latently infected neurons, the number of viral-genome copies in individual neurons, or both. It was found that within a defined range, a 2-log decrease in the input titer resulted in a statistically significant reduction in the number of latently infected neurons. Likewise as predicted, ACV treatment during the course of acute infection dramatically reduced the number of latently infected neurons.

For the first time, the number of viral genome copies within individual latently infected neurons has been examined. Although several investigators have calculated an average number of viral genomes by dividing the total viral-genome burden by the number of LAT-containing cells (13, 16, 35), it is now clear that the pool of latently infected neurons contain a variable number of viral genomes. From comparison to HSV standards, it is apparent that the majority of latently infected neurons contain fewer than 100 copies; a smaller percentage contain >100. Because the PCR assay is set up so that there is maximum linearity between 10 and 1,000 viral-genome copies, values above 1,000 genomes cannot be accurately quantified. The data indicates that a reduction in input titer shifts the greatest number of neurons into the <10-copies group, while an increase in titer results in the majority of neurons containing between 10 and 100 copies, although a more extensive analysis of these populations is required to reach statistical significance. ACV treatment had a profound effect on copy number. One hundred percent of the latent pool examined contained very low copy numbers, demonstrating that viral replication plays a role in generating latently infected neurons with a high viral-genome copy number.

CXA approaches add the opportunity to readily and accurately determine the latent viral burden of the host on a cellular basis to the arsenal of the molecular virologist. The ability to examine the viral DNA within individual infected cells provides the opportunity to analyze virus genome structure, integration, and replication. Combined with the potential to analyze not only the DNA, but also the RNA content of these individual cells (32), CXA will provide a new level of discrimination in the identification of viral and cellular genes required for the establishment, maintenance, and reactivation of latent infections. Subsequent investigation of the role of these gene products will significantly advance our understanding of the molecular mechanisms whereby viral and cellular functions regulate persistent and latent infections. This information may lead directly to new chemo- and immunotherapeutic strategies for the prevention and treatment of herpetic disease.

ACKNOWLEDGMENTS

This work was supported by Public Health Service grants AI32121 (from the National Institute of Allergy and Infectious Diseases) and NS25879 (from the National Institute of Neurological Disorders and Stroke) and a CHMCC Trustee Grant.

I sincerely thank R. L. Thompson, Ashley T. Haase, Steven M. Wolinsky, and William Sugden for helpful discussion and critical review of the manuscript; R. L. Thompson for use of mutant TB; and C. S. Tansky for expert technical assistance.

REFERENCES

1. **Ahmed, R., and J. G. Stevens.** 1990. Viral persistence, p. 241–265. *In* B. N. Fields (ed.), Virology. Raven Press, Ltd., New York, N.Y.
2. **Aldskogius, H., and J. Arvidsson.** 1978. Nerve cell degeneration and death in the trigeminal ganglion of the adult rat following peripheral nerve section. J. Neurocytol. **7:**229–250.
3. **Biedenbach, M. A., D. N. Kalu, and D. C. Herbert.** 1992. Effects of aging and food restriction on the trigeminal ganglion: a morphometric study. Mech. Ageing Dev. **65:**111–125.
4. **Coen, D. M., M. Kosz-Vnenchak, J. G. Jacobson, D. A. Leib, C. L. Bogard, P. A. Shaffer, K. L. Tyler, and D. M. Knipe.** 1989. Thymidine kinase-negative herpes simplex virus mutants establish latency in mouse trigeminal ganglia but do not reactivate. Proc. Natl. Acad. Sci. USA **86:**4736–4740.
5. **Davies, A., and A. Lumsden.** 1984. Relation of target encounter and neuronal death to nerve growth factor responsiveness in the developing mouse trigeminal ganglion. J. Comp. Neurol. **223:**124–137.
6. **Deatly, A. M., J. G. Spivack, E. Lavi, and N. W. Fraser.** 1987. RNA from an immediate early region of the type 1 herpes simplex virus genome is present in the trigeminal ganglia of latently infected mice. Proc. Natl. Acad. Sci. USA **84:**3204–3208.
7. **De Boni, U., and S. S. S. Goldenberg.** 1989. Isolation of pure fractions of viable dorsal root ganglionic neurons from rabbit or mouse using Percoll gradients, p. 230–232. *In* A. Shahar (ed.), A dissection and tissue culture manual of the nervous system. Alan R. Liss, New York, N.Y.
8. **Devi-Rao, G. B., D. C. Bloom, J. G. Stevens, and E. K. Wagner.** 1994. Herpes simplex virus type 1 DNA replication and gene expression during explant-induced reactivation of latently infected murine sensory ganglia. J. Virol. **68:**1271–1282.
9. **Ecob-Prince, M. S., C. M. Preston, F. J. Rixon, K. Hassan, and P. G. E. Kennedy.** 1993. Neurons containing latency-associated transcripts are numerous and widespread in dorsal root ganglia following footpad inoculation of mice with herpes simplex virus type 1 mutant in 1814. J. Gen. Virol. **74:**985–994.
10. **ElShamy, W. M., and P. Ernfors.** 1996. Requirement of neutrophin-3 for the survival of proliferating trigeminal ganglion progenitor cells. Development **122:**2405–2414.
11. **Field, H. J., S. E. Bell, G. B. Elion, A. A. Nash, and P. Wildy.** 1979. Effect of acycloguanosine treatment on acute and latent herpes simplex infections in mice. Antimicrob. Agents Chemother. **15:**554–561.
12. **Field, H. J., and E. De Clercq.** 1981. Effects of oral treatment with acyclovir and bromovinyldeoxyuridine on the establishment and maintenance of latent herpes simplex virus infection in mice. J. Gen. Virol. **56:**259–265.
13. **Hill, J. M., B. M. Gebhardt, R. Wen, A. M. Bouterie, H. W. Thompson, R. J. O'Callaghan, W. P. Halford, and H. E. Kaufman.** 1996. Quantitation of herpes simplex virus type 1 DNA and latency-associated transcripts in rabbit trigeminal ganglia demonstrates a stable reservoir of viral nucleic acids during latency. J. Virol. **70:**3137–3141.
14. **Hill, T. J.** 1985. Herpes simplex virus latency, p. 175–240. *In* B. Roizman (ed.), The herpesviruses. Plenum Press, New York, N.Y.
15. **Holland, G. R., and P. P. Robinson.** 1990. Cell counts in the trigeminal ganglion of the cat after inferior alveolar nerve injuries. J. Anat. **171:**179–186.
16. **Katz, J. P., E. T. Bodin, and D. M. Coen.** 1990. Quantitative polymerase chain reaction analysis of herpes simplex virus DNA in ganglia of mice infected with replication-incompetent mutants. J. Virol. **64:**4288–4295.
17. **Klein, R. J., and A. E. Friedman-Kein.** 1985. Effect of 9-(1,3-dihydroxy-2-propoxymethyl)guanine on the acute local phase of herpes simplex virus-induced skin infections in mice and the establishment of latency. Antimicrob. Agents Chemother. **27:**763–768.
18. **Kosz-Vnenchak, M., J. Jacobson, D. M. Coen, and D. M. Knipe.** 1993. Evidence for a novel regulatory pathway for herpes simplex virus gene expression in trigeminal ganglion neurons. J. Virol. **67:**5383–5393.
19. **Kramer, M. F., and D. M. Coen.** 1995. Quantification of transcripts from the ICP4 and thymidine kinase genes in mouse ganglia latently infected with herpes simplex virus. J. Virol. **69:**1389–1399.
20. **Laemmli, U. K.** 1970. Cleavage of structural proteins during the assembly of the head of bacteriophage T4. Nature (London) **227:**680–685.
21. **Leist, T. P., R. M. Sandri-Goldin, and J. G. Stevens.** 1989. Latent infections in spinal ganglia with thymidine kinase-deficient herpes simplex virus. J. Virol. **63:**4976–4978.
22. **Lessard, J.** 1988. Two monoclonal antibodies to actin: one muscle selective and one generally reactive. Cell Motil. Cytoskeleton **10:**349–362.
23. **Maggioncalda, J., A. Mehta, Y. H. Su, N. W. Fraser, and T. M. Block.** 1996. Correlation between herpes simplex virus type 1 rate of reactivation from latent infection and the number of infected neurons in trigeminal ganglia. Virology **225:**72–81.
24. **McLennan, J. L., and G. Darby.** 1980. Herpes simplex virus latency: the cellular location of virus in dorsal root ganglia and the fate of the infected cell following virus activation. J. Gen. Virol. **51:**233.
25. **Mehta, A., J. Maggioncalda, O. Bagasra, S. Thikkavarapu, P. Saikumari, T. Valyi-Nagy, N. W. Fraser, and T. M. Block.** 1995. *In situ* DNA PCR and RNA hybridization detection of herpes simplex virus sequences in trigeminal ganglia of latently infected mice. Virology **206:**633–640.
26. **Ramakrishnan, R., D. J. Fink, G. Jiang, P. Desai, J. C. Glorioso, and M. Levine.** 1994. Competitive quantitative PCR analysis of herpes simplex virus type 1 DNA and latency-associated transcript RNA in latently infected cells of the rat brain. J. Virol. **68:**1864–1873.
27. **Rock, D. L., W. A. Hagemoser, F. A. Osorio, and D. E. Reed.** 1986. Detection of bovine herpesvirus type 1 RNA in trigeminal ganglia of latently infected rabbits by *in situ* hybridization. J. Gen. Virol. **67:**2515–2520.
28. **Rock, D. L., A. B. Nesburn, H. Ghiasi, J. Ong, T. L. Lewis, J. R. Lokensgard, and S. L. Wechsler.** 1987. Detection of latency-related viral RNAs in tri-

geminal ganglia of rabbits latently infected with herpes simplex virus type 1. J. Virol. **61:**3820–3826.
29. **Roizman, B., and A. E. Sears.** 1990. Herpes simplex viruses and their replication, p. 1795–1841. *In* B. N. Fields (ed.), Virology. Raven Press, Ltd., New York, N.Y.
30. **Roizman, B., and A. E. Sears.** 1996. Herpes simplex viruses and their replication, p. 2231–2295. *In* B. N. Fields, D. M. Knipe, and P. M. Howley (ed.), Virology. Lippincott-Raven Publishers, Philadelphia, Pa.
31. **Sambrook, J., E. F. Fritsch, and T. Maniatis.** 1989. Molecular cloning: a laboratory manual. Cold Spring Harbor Laboratory Press, Cold Spring Harbor, N.Y.
32. **Sawtell, N. M.** Unpublished data.
32a. **Sawtell, N. M., and T. M. Block.** Unpublished data.
33. **Sawtell, N. M., and J. M. Lessard.** 1989. Cellular distribution of smooth muscle actins during mammalian embryogenesis: expression of the alpha-vascular but not the gamma-enteric isoform in differentiating striated myocytes. J. Cell Biol. **109:**2929–2937.
34. **Sawtell, N. M., and R. L. Thompson.** 1992. Rapid *in vivo* reactivation of herpes simplex virus in latently infected murine ganglionic neurons after transient hyperthermia. J. Virol. **66:**2150–2156.
35. **Sawtell, N. M., and R. L. Thompson.** 1992. Herpes simplex virus type 1 latency-associated transcription unit promotes anatomical site-dependent establishment and reactivation from latency. J. Virol. **66:**2157–2169.
36. **Sedarati, F., K. M. Izumi, E. K. Wagner, and J. G. Stevens.** 1989. Herpes simplex virus type 1 latency-associated transcription plays no role in establishment or maintenance of a latent infection in murine sensory neurons. J. Virol. **63:**4455–4458.
37. **Sedarati, F., T. P. Margolis, and J. G. Stevens.** 1993. Latent infection can be established with drastically restricted transcription and replication of the HSV-1 genome. Virology **192:**687–691.
38. **Stevens, J. G.** 1989. Herpes simplex virus latency analyzed by *in situ* hybridization. Curr. Top. Microbiol. Immunol. **143:**1–8.
39. **Stevens, J. G., E. K. Wagner, G. B. Devi-Rao, M. L. Cook, and L. T. Feldman.** 1987. RNA complementary to a herpesvirus alpha gene mRNA is prominent in latently infected neurons. Science **235:**1056–1059.
40. **Stroop, W. G., D. L. Rock, and N. W. Fraser.** 1984. Localization of herpes simplex virus in the trigeminal and olfactory systems of the mouse central nervous system during acute and latent infections by *in situ* hybridization. Lab. Invest. **51:**27–38.
41. **Tenser, R. B., M. Dawson, S. J. Ressel, and M. E. Dunstan.** 1982. Detection of herpes simplex virus mRNA in latently infected trigeminal ganglion neurons by *in situ* hybridization. Ann. Neurol. **11:**285–291.
42. **Tenser, R. B., W. A. Edris, and K. A. Hay.** 1989. Herpes simplex latent infection: quantitation of latency-associated transcript-positive neurons and reactivable neurons. Yale J. Biol. Med. **62:**197–204.
43. **Thackray, A. M., and H. J. Field.** 1996. Differential effects of famciclovir and valaciclovir on the pathogenesis of herpes simplex virus in a murine infection model including reactivation from latency. J. Infect. Dis. **173:**291–299.
44. **Thompson, R. L., S. K. Rogers, and M. A. Zerhusen.** 1989. Herpes simplex virus neurovirulence and productive infection of neural cells is associated with a function which maps between 0.82 and 0.832 map units on the HSV genome. Virology **172:**435–450.
45. **Thompson, R. L., and N. M. Sawtell.** 1997. The herpes simplex virus type 1 latency-associated transcript gene regulates the establishment of latency. J. Virol. **71:**5432–5440.
46. **Towbin, H., T. Staehelin, and J. Gordon.** 1979. Electrophoretic transfer of proteins from polyacrylamide gels to nitrocellulose sheets: procedure and some applications. Proc. Natl. Acad. Sci. USA **76:**4350–4354.
47. **Walz, M. A., R. W. Price, and A. L. Notkins.** 1974. Latent ganglionic infection with herpes simplex virus types 1 and 2: viral reactivation *in vivo* after neurectomy. Science **184:**1185–1187.
48. **Waymouth, C.** 1982. Methods for obtaining cells in suspension from animal tissues. *In* T. G. Pretlow II and T. P. Pretlow (ed.), Cell separation: methods and selected applications. Academic Press, New York, N.Y.